Limnol. Oceanogr., 53(5), 2008, 1878–1886
© 2008, by the American Society of Limnology and Oceanography, Inc.

Ballast, sinking velocity, and apparent diffusivity within marine snow and zooplankton fecal pellets: Implications for substrate turnover by attached bacteria

Helle Ploug[1] *and Morten Hvitfeldt Iversen*
Alfred Wegener Institute for Polar and Marine Research, Am Handelshafen 12, D-27570 Bremerhaven, Germany

Gerhard Fischer
Dept. of Geosciences, University of Bremen, Klagenfurther Str., D-28357 Bremen, Germany;
Research Center Ocean Margins (RCOM), Leobener Str., D-28359 Bremen, Germany

Abstract

We analyzed size-specific dry mass, sinking velocity, and apparent diffusivity in field-sampled marine snow, laboratory-made aggregates formed by diatoms or coccolithophorids, and small and large zooplankton fecal pellets with naturally varying content of ballast materials. Apparent diffusivity was measured directly inside aggregates and large (millimeter-long) fecal pellets using microsensors. Large fecal pellets, collected in the coastal upwelling off Cape Blanc, Mauritania, showed the highest volume-specific dry mass and sinking velocities because of a high content of opal, carbonate, and lithogenic material (mostly Saharan dust), which together comprised ~80% of the dry mass. The average solid matter density within these large fecal pellets was 1.7 g cm^{-3}, whereas their excess density was 0.25 ± 0.07 g cm^{-3}. Volume-specific dry mass of all sources of aggregates and fecal pellets ranged from 3.8 to 960 μg mm^{-3}, and average sinking velocities varied between 51 and 732 m d^{-1}. Porosity was >0.43 and >0.96 within fecal pellets and phytoplankton-derived aggregates, respectively. Averaged values of apparent diffusivity of gases within large fecal pellets and aggregates were 0.74 and 0.95 times that of the free diffusion coefficient in sea water, respectively. Ballast increases sinking velocity and, thus, also potential O_2 fluxes to sedimenting aggregates and fecal pellets. Hence, ballast minerals limit the residence time of aggregates in the water column by increasing sinking velocity, but apparent diffusivity and potential oxygen supply within aggregates are high, whereby a large fraction of labile organic carbon can be respired during sedimentation.

Marine snow and fecal pellets comprise a significant fraction of the sinking carbon flux in the ocean (Alldredge and Silver 1988; Simon et al. 2002; Turner 2002). Hence, sedimentation of these particles into the bathypelagic zone is important for the ocean's capacity to sequester CO_2 from the atmosphere, i.e., the ocean's biological carbon pump (De La Rocha and Passow 2007). The recent observation that carbonate and organic carbon fluxes show close correlations in the bathypelagic zone of the ocean has led to the hypothesis that biominerals in phytoplankton, e.g., carbonate and opal, promote carbon preservation of the sinking flux because these biominerals increase sinking velocity because of their high densities and/or protect a fraction of the organic matter in the cells from being degraded in the deep ocean (Armstrong et al. 2002; Francois et al. 2002; Klaas and Archer 2002). The effect of ballast minerals on sinking velocity relative to that on small-scale oxygen fluxes and degradation rates in sinking particles, however, is largely unknown.

The physical and chemical microenvironment of sinking particles is significantly different from that of the surrounding water. High concentrations of inorganic and organic matter, ecto-enzymatic activities, and remineralization rates by attached bacteria lead to oxygen and pH gradients within sinking marine snow and fecal pellets (Alldredge and Cohen 1987; Smith et al. 1992; Ploug et al. 1999). The observations that dissolved organic carbon (DOC), silicic acid, ammonium, and phosphate concentrations are higher inside marine snow compared to the surrounding water have led to the hypothesis that diffusion within marine snow is significantly slower than in sea water (Shanks and Trent 1979; Brzezinski et al. 1997; Alldredge 2000).

The flux of a solute within an aggregate equals the product of the apparent diffusivity and the radial concentration gradient of the solute, i.e., Fick's first law of diffusion:

$$J = \phi D_s \frac{dC}{dr} \quad (1)$$

where J is the flux of the solute, ϕ is the porosity, D_s is the effective diffusion coefficient, and dC/dr is the radial concentration gradient of the solute. The combined parameter (ϕD_s) is the apparent diffusivity of the solute. The effective diffusion coefficient is a function of porosity,

[1] Corresponding author (Helle.Ploug@awi.de).

Acknowledgments

The oxygen microelectrodes were constructed by Gaby Eickert, Ines Schröder, and Karin Hohmann, Max Planck Institute for Marine Microbiology, Bremen. We thank Thomas Kiørboe for providing laboratory facilities to measure fecal pellet sinking velocity. We also thank Christine Klaas and two anonymous reviewers for critical comments that improved the manuscript.

This study was funded by the Helmholtz Association (to H.P.), the Alfred Wegener Institute for Polar and Marine Research, and the Deutsche Forschungsgemeinschaft as part of the DFG-Research Center "Ocean Margins" of the University of Bremen MARUM 0570.

tortuosity, and the free diffusion coefficient in water (D_0). The tortuosity relates the actual distance a molecule or an ion travels within an aggregate to the distance it travels in water per unit length of the aggregate. Direct measurements of apparent diffusivity in marine snow are scarce. Recently, apparent diffusivity of gases was measured directly within diatom aggregates containing transparent exopolymer particles (TEP) using a microsensor (Ploug and Passow 2007). Apparent diffusivity of gases within these aggregates was close to the free molecular diffusion coefficient of these in the surrounding water, independently of size and age of the aggregates. Steep concentration gradients of oxygen within diatom aggregates thus reflected high biological activity (fluxes) within these aggregates rather than low diffusivity.

In the present study, we analyze the effect that ballast has on sinking velocity, apparent diffusivity, and small-scale oxygen fluxes to sinking particles of different sources with naturally varying content of ballast material, e.g., field-sampled marine snow; laboratory-made aggregates formed by diatoms or coccolithophorids; and small and large zooplankton fecal pellets, containing biogenic and/or lithogenic ballast minerals.

Methods

Aggregates and fecal pellets—Cultures of diatoms (*Skeletonema costatum*) and coccolithophorids (*Emiliania huxleyi*) were grown at 15°C in F/2 medium in a 12 : 12 light : dark cycle during 14–28 d (Guillard and Ryther 1962). Aggregates of the respective cultures were formed in roller tanks rotating at 3 rounds min^{-1} in darkness (Shanks and Edmonson 1989). Diatom aggregates formed during the first day after the culture had been transferred to roller tanks. Aggregates from the coccolithophorid culture formed only after 5 d of rotation. Large zooplankton fecal pellets, most probably produced by giant mesopelagic larvaceans (appendicularians), had been collected in sediment traps from 1,296-m water depth from the eutrophic site CBi-2 off Cape Blanc, Mauritania, NW Africa (20°45′N, 18°42′W). The sample cups were filled with filtered seawater and poisoned with $HgCl_2$ before deployment. The coastal upwelling area is characterized by high production of coccolithophorids and diatoms, and a high input of dust from the Sahara (Fischer et al. in press). The fecal pellets (up to 1.5 mm in length) were pipetted individually from three sediment trap samples collected from 10 November 2004 to 18 January 2005 (sampling intervals 23 d each). Copepod fecal pellets were produced in culture experiments using *Temora longicornis* grown on *E. huxleyi* as previously described (Ploug et al. 2008).

Size measurements—Aggregates and large fecal pellets were placed on a net in a vertical flow system, and their size was determined under the dissection microscope using a calibrated ocular meter (Ploug and Jørgensen 1999). The aggregate or fecal pellet was turned during measurement, which allowed for size determination of all three axes. The dimensions of small fecal pellets were determined directly under a dissection microscope. The volume of aggregates was calculated assuming an ellipsoid, $V = (1/6)\ \pi \times \text{length} \times \text{width} \times \text{height}$, and that of fecal pellets was calculated assuming cylindrical geometry.

Dry mass and fractal dimension—Single aggregates or single appendicularian fecal pellets with known volumes were filtered onto preweighed 0.4-μm polycarbonate filters, washed and dried at 60°C for 48 h, and reweighed. Copepod fecal pellets were pooled in triplicate samples with 600 pellets $filter^{-1}$. The volume of 30 copepod fecal pellets was calculated from their dimensions. The sensitivity of the scale was 0.1 μg (Mettler Toledo, UMX 2). The fractal dimension (D_3) of aggregates was estimated from the relative distribution of mass in aggregates of different sizes measured as equivalent spherical diameter (Logan and Wilkinson 1990).

Sinking velocity—Aggregate sinking velocity was measured in a vertical flow system wherein an upward-directed flow velocity was adjusted to balance the sinking velocity of aggregates (Ploug and Jørgensen 1999). The sinking velocity was calculated from the volume of water passing through the flow chamber per unit time divided by the cross-sectional area of the flow chamber. An advantage of this method is that the aggregate is not destroyed and can easily be collected for further analysis afterwards. However, a comparison of aggregate sinking velocities measured within this flow system with those measured in a sedimentation column have shown that sinking velocities tend to be underestimated by 18% in the flow system relative to the values obtained in a sedimentation column (H. Ploug unpubl.). Sinking velocities were corrected by this value in the present study to normalize sinking velocity data to those measured in a sedimentation column (*see* below).

Fecal pellets do not disaggregate as easily as do marine snow and other porous aggregates. Sinking velocities of appendicularian fecal pellets were too high to be measured in the flow system because of air-bubble formation within the system at the high inflow rates needed to keep particles in suspension. Sinking velocities of fecal pellets were therefore measured in a sedimentation column. The column (40 cm high and 3 cm in diameter) was filled with filtered seawater (~32) and kept in a 15°C thermostated room, surrounded by a water jacket for thermal stabilization. The settling column was closed at both ends, allowing only insertion of a Pasteur pipette at the top. Pellets were rinsed in filtered seawater and collected in a Pasteur pipette with filtered seawater (~32). Pellets sank out of the Pasteur pipette, which was centered in the column. The descent of the pellets was recorded by two charge-coupled device video cameras (MTV-1802CB, Mintron) equipped with 105-mm lenses (Micro Nikkor 1 : 2.8, Nikon). The cameras were placed along the *x*- and *z*-axes of the pellets, giving a three-dimensional view of the settling. A time-code generator was connected to the cameras, making timing of the pellets possible. Infrared illumination was provided from behind by light-emitting diodes and collimated through condensers. The setup was

calibrated by recording a length scale before sinking velocity measurements.

Theoretical sinking velocities of aggregates and fecal pellets were calculated from

$$U = \left(2g\Delta\rho V / \rho_f C_D A\right)^{0.5} \quad (2)$$

where U is the sinking velocity, g is the acceleration caused by gravity, $\Delta\rho$ is the excess density of the aggregates, and ρ_f is the density of sea water (1.02488 g at 15°C). C_D is the drag coefficient and A is the cross-sectional area of the particle.

The Reynolds number was calculated as (White 1974)

$$Re = \frac{dU}{v} \quad (3)$$

where d is the diameter and v is the kinematic viscosity of sea water (1.19×10^{-2} cm^2 s^{-1} at 15°C).

The drag coefficient for $Re > 0.5$ was calculated as (White 1974)

$$C_D = \frac{24}{Re} + \frac{6}{1 + Re^{0.5}} + 0.4 \quad (4)$$

Excess density and solid matter density—The excess density of aggregates was calculated from measured sinking velocities (Eq. 2) using the drag coefficient (Eq. 4). The solid matter density was calculated from Alldredge and Gotschalk (1988):

$$\Delta\rho = \frac{W}{V} \times \left(1 - \frac{\rho_f}{\rho_s}\right) \quad (5)$$

where W is the dry mass, ρ_s the solid matter density, and V the volume of the aggregate.

The densities of fecal pellets were determined experimentally in a density gradient, using a modified version of the centrifugation method (Schwinghamer et al. 1991; Feinberg and Dam 1998). Seven dilutions were made using Ludox TM colloidal silica, sucrose, and distilled water. The dilutions ranged in density from 1.05 to 1.43 g cm^{-3}. The dilutions were buffered to pH 8.1 with 0.0125 mol L^{-1} Tris plus 0.0125 mol L^{-1} Tris-HCl (final concentration). Hence, the gradient produced was isosmotic with seawater of salinity ~32 (Weast 1968). Two milliliters of each dilution was gently transferred to a 20-mL centrifuge tube, beginning with the densest and finishing with the lightest dilution. The density gradients were stored at 5°C overnight but were at room temperature before use. Whole fecal pellets were rinsed in filtered seawater (~32), placed in 1 mL of seawater, and pipetted on top of the density gradient. The samples were centrifuged at 3,000 rpm for 30 min. After centrifugation, 1 mL from each of the different density layers was removed from the tube using a peristaltic pump and weighed using a Mettler Toledo balance to 0.1 mg. The size and number of pellets layer^{-1} were recorded using a dissection microscope. No pellets were observed to be disrupted by the centrifugation process.

Porosity—The porosity of aggregates and fecal pellets was calculated as (Alldredge and Gotschalk 1988):

$$p = 1 - \frac{W/\rho_s}{V} \quad (6)$$

The calculated porosity in aggregates is relatively insensitive to the density of dry mass because aggregate porosity is very high, as also previously noted by Alldredge and Gotschalk (1988).

Scanning electron microscopy—Aggregate or fecal pellet composition was visually analyzed using scanning electron microscopy (SEM). Aggregates and fecal pellets were filtered onto 0.4-μm polycarbonate filters, rinsed with deionized water, and dried >24 h at 40°C. The filters were covered with a 5-nm gold–palladium layer (SC500, Emscope). Random areas of the filters were chosen for visual determination of the content. SEM analysis was performed using an FEI Quanta 200F scanning electron microscope together with xTmicroscope software.

Elemental analysis of fecal pellets—About 50 appendicularian pellets were collected with a pipette from the wet splits (1/5) from three samples from the CBi-2 trap positioned at 1,296-m water depth. Pellets were freeze-dried and homogenized with a mortar. We performed organic carbon, total nitrogen, and carbonate analysis using a HERAEUS-CHN analyzer. Organic carbon was measured using the freeze-dried material, from which calcium carbonate was removed with 6 mol L^{-1} HCl in silver boats and dried on a hot plate prior to the analysis. Carbonate was determined from the difference between nonacidified samples and acidified samples. Biogenic opal was determined with a sequential leaching technique with 1 mol L^{-1} NaOH (Müller and Schneider 1993). Lithogenic material was calculated according to: lithogenic = total mass – opal – calcium carbonate – 2 × organic carbon. Organic carbon was multiplied by a factor of 2 to estimate total organic matter (Wakeham et al. 1980).

Diffusivity—Apparent diffusivity was measured directly within aggregates or fecal pellets using a diffusivity microsensor (Unisense) connected to a picoammeter (PA2000, Unisense) and a strip chart recorder (Revsbech et al. 1998; Ploug and Passow 2007). The detection principle is based on a tracer gas (hydrogen) diffusing away from the microsensor tip. These sensors are very stable. Hydrogen, however, is not a completely inert gas in biological systems. Production or consumption of hydrogen can be recognized by non–steady-state signals within biological samples. Such signals were never observed during our measurements. The microsensor was attached to a micromanipulator. The tip diameter was 50 μm and its position was observed under a dissection microscope. The microsensor was calibrated in glass beads with a diameter of 5–20 μm, and in stagnant water in the boundary layer of a piece of 1% agar (Revsbech et al. 1998; Ploug and Passow 2007). Single aggregates or fecal pellets were placed on a net to ensure free diffusion in all dimensions during measurements, i.e., to avoid wall effects (Ploug and

Table 1. Source and culture age, sample size, equivalent spherical diameter (*ESD*), volume-specific dry mass (Vol.-spec. dry mass), fractal dimension (D_3), porosity, apparent diffusivity ($\phi D_s : D_0$) within aggregates, sinking velocity (U), and Sherwood number (Sh) for marine snow, phytoplankton-derived aggregates, and fecal pellets (fp). nd: no data.

Source	No. in sample	*ESD* (mm)	Vol.-spec. dry mass (μg mm^{-3})	D_3	Porosity	$\phi D_s : D_0$	U (m d^{-1})	*Sh*
Marine snow*	12	2.9±1.3	3.8±1.0	nd	0.996	nd	51±56	5.9
S. costatum (2 weeks)	35	2.8±0.5	8.3±2.8	1.60±0.22	0.992±0.003	0.95±0.01	140±41	8.3
S. costatum (5 weeks)	22	2.0±0.7	9.3±5.3	1.47±0.22	0.989±0.009	nd	250±97	9.0
S. costatum (2 weeks)	12	1.7±0.3	16.2±4.5	1.63±0.18	0.984±0.004	0.95±0.01	80±26	5.9
E. huxleyi (3 weeks)	12	1.5±0.3	44±19	2.16±0.82	0.959±0.018	0.95±0.02	216±31	7.7
Appendicularian fp	38	0.63±0.09	960±171†	—	0.434±0.100†	0.74±0.06†	732±153	8.8
Copepod fp	20	0.10±0.02	550‡	—	0.65	nd	199±92	3.1

* Collected in the Southern California Bight (Ploug et al. 1999).
† n=7.
‡ 3×600 pooled fp.

Jørgensen 1999; Ploug and Passow 2007). The apparent diffusivity was measured at multiple positions within each aggregate or fecal pellet at stagnant conditions. After measurements, aggregates and fecal pellets were further processed for dry mass measurements.

Oxygen measurements—Oxygen distributions were measured within and around marine snow and phytoplankton-derived aggregates using a microelectrode with a tip diameter of 10 μm attached to a micromanipulator (Revsbech 1989). The microsensor was calibrated at air saturation and under anoxic conditions. Its 90% response time was <1 s, and its stirring sensitivity was <0.3%. Its current was read by a picoammeter connected to a strip chart recorder. The aggregate was placed on a net in the vertical flow system and the flow was adjusted to suspend the aggregate one diameter above the net, whereby its sinking velocity was balanced by the upward-directed flow velocity (Ploug and Jørgensen 1999; Kiørboe et al. 2001). The microelectrode was slowly brought to the aggregate surface as observed under the dissection microscope. The gradients across the aggregate–water interface were measured at 50–100-μm depth increments, and afterwards analyzed using a diffusion-reaction model to calculate the oxygen uptake rates and to estimate the apparent diffusivity inside aggregates (Ploug et al. 1997). This model is based on mass balance of fluxes at the aggregate–water interface assuming aggregates to be impermeable to flow. The flux of oxygen into the aggregate, which is the product of the apparent diffusivity and the oxygen concentration gradient below the aggregate surface, must equal the diffusive supply from the surrounding water at the aggregate–water interface. This model has previously been shown to give very accurate estimates of oxygen uptake in model systems like agar beads (Ploug et al. 2002).

The Sherwood number for oxygen transport to sinking aggregates and fecal pellets was calculated as (Kiørboe et al. 2001)

$$Sh = 1 + 0.619 \times \left(\frac{Ur_0}{\nu}\right)^{0.421} \left(\frac{\nu}{D_0}\right)^{1/3} \quad (7)$$

where r_0 is the aggregate radius (cm) and D_0 is the molecular diffusion coefficient of oxygen in sea water (1.74×10^{-5} cm^2 s^{-1} at 15°C; Broecker and Peng 1974).

Results

Equivalent spherical diameter, volume-specific dry mass, fractal dimension (D_3), porosity, apparent diffusivity ($\phi D_s : D_0$), sinking velocity (U), and Sherwood number (Sh) in marine snow, phytoplankton-derived aggregates, and fecal pellets are summarized in Table 1. The diameters varied approximately 30-fold across the different sources of aggregates and fecal pellets. The porosity of field-sampled marine snow and of aggregates derived from phytoplankton cultures was high (>0.95). Volume-specific dry mass, porosity, sinking velocity, and Sherwood number of diatom aggregates varied greatly depending on average aggregate size and age as observed in our three diatom cultures (*S. costatum*). The densest and most compact phytoplankton aggregates were those formed from the *E. huxleyi* culture. These aggregates had on average a higher fractal dimension and lower porosity compared to those formed by the diatom. Scanning electron microscopy showed that these aggregates had a very high content of liths. The volume-specific dry mass in appendicularian fecal pellets was approximately 250-fold higher than that in field-sampled marine snow. Forty-four percent of their dry mass was lithogenic material (mostly Sahara dust), 27% was calcium carbonate, and organic carbon comprised 12% of the dry mass content (Table 2). The mean C_{org} : N ratio was 11. The estimated porosity was significantly lower in fecal pellets compared to that measured in phytoplankton-derived aggregates and marine snow. Apparent diffusivity within phytoplankton aggregates was close to the free diffusion coefficient in sea water in contrast to that within appendicularian fecal pellets, which was significantly lower than the free diffusion coefficient in sea water (Table 1). Sinking velocity varied up to 14-fold for different sizes and sources of aggregates. Estimated excess densities varied more than 1,000-fold. The estimated solid matter density varied between 1.08 and 1.7 g cm^{-3} (Table 3).

The Sherwood number measures the enhancement of mass transfer (diffusion and advection) to a sinking particle relative to that to a stagnant particle (diffusion only) in the water column. Hence, the potential mass transfer to sinking aggregates and fecal pellets was enhanced 3- to 9-fold compared to that to stagnant aggregates and pellets. The

Table 2. Average composition (in % of dry mass with the standard deviation of the mean value; $n=3$) of appendicularian fecal pellets collected in sediment traps (1,296-m water depths) off Cape Blanc, Mauritania, from 10 November 2004 to 18 January 2005.

	Composition
C_{org}	12±2.7
Nitrogen	1.31±0.37
Calcium carbonate	27±8
Biogenic opal	8.8±0.4
Lithogenic material	44±6

potential mass transfer of oxygen to denser and faster-sinking aggregates was enhanced by 31–41% relative to that to similar-sized aggregates with lower density and sinking velocity (Table 1). Diatom aggregates formed by an older culture showed higher sinking velocities compared to those formed by the younger one, although the average dry mass (wet volume)$^{-1}$ was similar in aggregates of the two cultures.

The fluxes of oxygen to sinking aggregates are determined by the potential mass transfer of oxygen by diffusion and/or advection and by the oxygen consumption rates within aggregates. The oxygen gradients within aggregates, which are not permeable to fluid flow, depend on aggregate size, oxygen consumption rates, the apparent diffusivity within aggregates, and the concentration boundary layer thickness at the aggregate–water interface during sinking, i.e., the Sherwood number (Ploug et al. 1997; Ploug 2001). Here, we estimated the apparent diffusivity of oxygen within aggregates and marine snow from measured oxygen gradients using a diffusion-reaction model assuming our aggregates to be impermeable to flow. Three examples of oxygen gradients measured in field-sampled marine snow (Ploug et al. 1999), diatom aggregates, and aggregates formed by the *E. huxleyi* culture are shown in Fig. 1. The oxygen consumption rates in the aggregates were calculated from the oxygen gradient in the water phase immediately adjacent to the aggregate surface, i.e., they can be determined independently of the apparent diffusivity inside the aggregates, because all oxygen being consumed inside the aggregate must cross the aggregate–water interface. The measured oxygen gradients were consistent with those modeled for similar-sized aggregates with an apparent diffusivity of oxygen within the aggregate of 0.95 times the free diffusion coefficient of oxygen in sea water in all three cases. The variation in oxygen gradients between aggregates was explained by variations in oxygen consumption rates. The oxygen consumption rate in field-sampled marine snow was 2.3 nmol O_2 h^{-1}, whereas that of the diatom aggregate was 4.6 nmol O_2 h^{-1}, and that of the aggregate formed by the *E. huxleyi* culture was 14.3 nmol O_2 h^{-1}. Hence, aggregates formed by the *E. huxleyi* culture were rich in liths as well as in labile organic matter. Assuming an apparent diffusivity of oxygen within aggregates to be 0.1 or 0.01 times that of the free diffusion coefficient in sea water resulted in significantly different oxygen gradients compared to those measured within the aggregates (Fig. 2). The aggregates would have been anoxic if the apparent diffusivity had been only 1–10% of the free diffusion coefficient. Diffusion of oxygen, therefore, did not limit the bacterial respiration of organic matter within these aggregates.

Discussion

Sinking velocity and remineralization rates of particles are two major factors determining vertical carbon fluxes and the efficiency of the biological carbon pump in the ocean (De La Rocha and Passow 2007). Phytoplankton-derived aggregates and zooplankton fecal pellets are important components in the vertical carbon flux to the deep sea and sediments (Turner 2002). The present study is the first to directly measure aggregate or fecal pellet composition, density, sinking velocity, apparent diffusivity, and O_2 fluxes across a variety of particle sources occurring in the ocean. Hereby we could experimentally assess the effect of ballast on sinking velocities and mineralization rates of phytoplankton-derived aggregates and fecal pellets in the upper ocean. We used volume-specific dry mass, excess density, and solid matter density as measures of ballast, where chemical composition was not measured directly. The volume-specific dry mass varied 250-fold across the different particle and aggregate sources. It was shown that ballast minerals have little influence on

Table 3. Source and culture age, excess density, solid matter density (ρ_s), Reynolds number (Re), drag coefficient (C_D), theoretical sinking velocity (U_{theory}), and the ratio between measured and theoretical sinking velocity. fp: fecal pellet.

Source	Excess density (mg cm^{-3})	ρ_s (g cm^{-3})	Re	C_D	U_{theory} (m d^{-1})	$U: U_{theory}$
Marine snow*	0.19†	1.08	1.43	20	52	0.98
S. costatum (2 weeks)	0.63†	1.11	3.81	3.8	139	1.00
S. costatum (5 weeks)	2.23†	1.35	4.86	4.9	243	1.03
S. costatum (2 weeks)	0.83†	1.08	1.32	1.3	79	1.01
E. huxleyi (3 weeks)	3.36†	1.11	3.15	3.2	217	0.99
Appendicularian fp	250±70	1.7	4.48	4.5	1,233	0.59
Copepod fp	150±40	1.6	0.19	0.20	105	1.88

† Calculated from measured sinking velocity (Eq. 2).
* Collected in the Southern California Bight (Ploug et al. 1999).

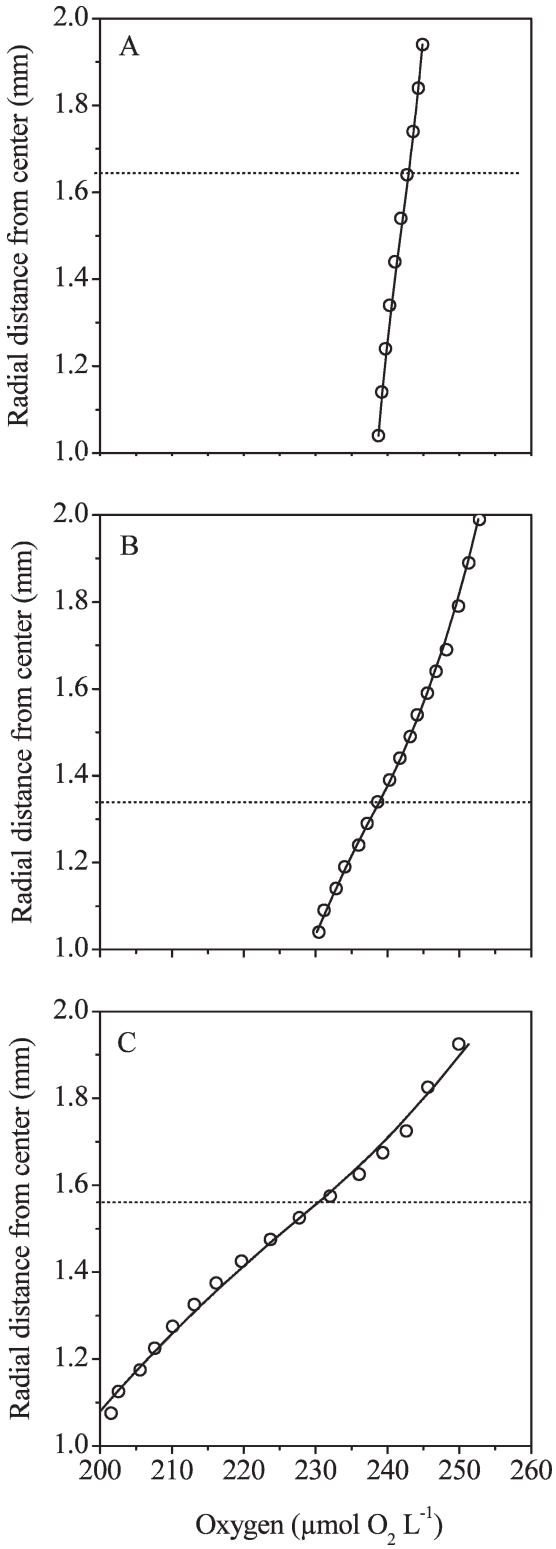

Fig. 1. (A) Oxygen gradients measured (circles) and modeled (line) across the aggregate–water interface assuming an apparent diffusivity of oxygen to be 0.95 times the free diffusion coefficient inside sea water in marine snow, (B) an aggregate formed by *S. costatum*, and (C) an aggregate formed by *E. huxleyi*. The horizontal dotted lines indicate the aggregate surface. *See* text for details.

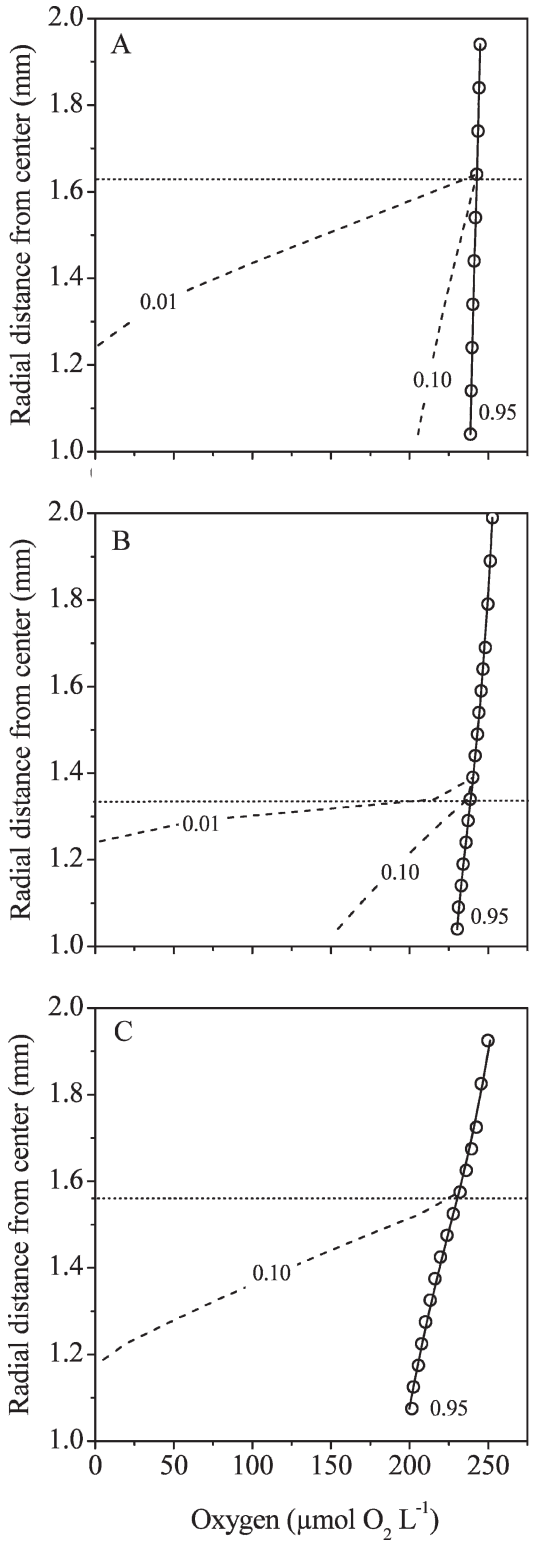

Fig. 2. (A) Oxygen gradients measured (circles) and modeled (line) across the aggregate–water interface assuming an apparent diffusivity of oxygen to be 0.95, 0.10, or 0.01 times the free diffusion coefficient in sea water inside marine snow, (B) an aggregate formed by *S. costatum*, and (C) an aggregate formed by *E. huxleyi*. The horizontal dotted lines indicate the aggregate surface. *See* text for details.

apparent diffusivity within aggregates, but these minerals increase sinking velocity and thereby also the potential O_2 fluxes to sedimenting aggregates and fecal pellets.

Sinking velocities of fecal pellets and marine snow cannot be predicted by Stokes' law, because their Reynolds numbers are well above 0.5, their geometry is nonspherical, and marine snow is porous. Furthermore, sinking velocities of similar-sized aggregates vary greatly (Alldredge and Gotschalk 1988; Khelifa and Hill 2007; Ploug et al. 2008). Our study demonstrates that sinking velocities of different particle types depend on source, density, and age rather than on size. Sinking velocity of similar-sized aggregates and fecal pellets is largely controlled by excess density, which depends on solid matter density, i.e., composition of primary particles, porosity, and fractal dimension (Khelifa and Hill 2007). A high content of lithogenic material (mostly fine-grained dust) and calcium carbonate in zooplankton fecal pellets coincides with high densities and sinking velocities of these pellets. By comparison, the excess density of large, porous phytoplankton-derived aggregates is much lower than that of fecal pellets. TEP are significant components in phytoplankton aggregates, where they occupy a high fraction of the aggregate volume but contribute little to dry mass (Ploug and Passow 2007). TEP can diminish sinking velocity of aggregates because of low specific density of these particles (Engel and Schartau 1999; Azetsu-Scott and Passow 2004). The TEP : dry mass ratio tends to decrease in aging aggregates, which may partly explain the increased sinking velocities and apparently higher solid matter densities in older aggregates of the present study (Ploug and Passow 2007).

It has been argued that diffusivity of gases and solutes within marine snow may be significantly lower than the respective diffusion coefficients in water because of their fractal geometry (Alldredge 2000). The fractal dimensions of our aggregates were similar to those reported from the field (Alldredge and Gotschalk 1988; Logan and Wilkinson 1990), but the apparent diffusivity of gases within porous marine snow and phytoplankton-derived aggregates was only slightly lower than that in (stagnant) sea water. High concentrations of cells, minerals, and TEP may limit advection rather than diffusion within aggregates. The apparent diffusivity in large fecal pellets with a very high volume-specific content of carbonate and lithogenic material was only approximately 25% lower than that in sea water. Although ballast material had little influence on apparent diffusivity within aggregates and fecal pellets, it had a large effect on sinking velocity and thus total mass transfer (diffusion and advection) of oxygen to sinking particles. Hence, our study provides no evidence for protection mechanisms against degradation of labile organic matter that might result from a lower diffusivity because of packaging of aggregates and fecal pellets during sedimentation.

It has previously been shown that millimeter-long euphausidian fecal pellets attached to marine snow can be anoxic (Alldredge and Cohen 1987). The aggregates analyzed in the present study were far from being anoxic. The half-saturation constant for oxygen uptake in bacteria is approximately 1 μmol L^{-1} (Fenchel and Finlay 1993), and bacterial respiration was thus not limited by oxygen availability within aggregates. The oxygen gradients occurring within the aggregates of our study were explained by the oxygen consumption rates in combination with a high apparent diffusivity of oxygen. This was also the case in anoxic aggregates formed by zooplankton detritus produced on a nanoflagellate diet (Ploug et al. 1997). Anoxic aggregates and particles, however, may be common within oxygen minimum zones with <25 μmol O_2 L^{-1}, rather than in fully oxygenated sea water (Ploug 2001, 2008).

Production, degradation, and residence time of organic carbon in sinking particles are complex processes that depend on physical processes, e.g. turbulence, as well as on chemical and biological processes in the upper mixed layer of the ocean. Macrocrustacean fecal pellets can remain in surface water much longer than could be expected from their sinking velocity alone (Alldredge et al. 1987). Marine snow and fecal pellets can disaggregate because of fragmentation by zooplankton, leading to decreased sinking velocities and increased substrate turnover within the upper mixed layer of the ocean (Dilling and Alldredge 2000; Iversen and Poulsen 2007). Bacteria associated with marine snow and fecal pellets are characterized by high enzymatic activities (Smith et al. 1992; Thor et al. 2003; Ziervogel and Arnosti 2008), leading to microenvironments with elevated concentrations of DOC, inorganic nutrients, and amino acids relative to those of the surrounding water (Smith et al. 1992; Brzezinski et al. 1997; Alldredge 2000). These microenvironments are 10- to 100-fold larger than the volume of sinking aggregates themselves because of advection and diffusion acting at the aggregate–water interface (Kiørboe et al. 2001; Ploug and Passow 2007). Chemosensory behavior has been demonstrated in marine bacteria as well as in zooplankton that feed on marine snow (Kiørboe 2001; Kiørboe et al. 2002). Hence, bacterial colonization of sinking marine particles is a very fast process leading to a significant turnover of the aggregate carbon and nitrogen pools in the surface ocean (Smith et al. 1992; Ploug et al. 1999; Kiørboe et al. 2002). Carbon-specific respiration rates are relatively similar within copepod fecal pellets, irrespective of biogenic ballast material content, and within marine snow (0.08 to 0.21 d^{-1}) (Ploug et al. 1999; Ploug and Grossart 2000; Ploug et al. 2008). This observation may largely be explained by high hydrolysis rates combined with high apparent diffusivities of solutes and oxygen supply for respiration, which support an efficient turnover of labile carbon across different particle sources and sizes in the ocean.

References

Alldredge, A. L. 2000. Interstitial dissolved organic carbon (DOC) concentrations within sinking marine aggregates and their potential contribution to carbon flux. Limnol. Oceanogr. **45:** 1245–1253.

———, and Y. Cohen. 1987. Can microscale chemical patches persist in the sea? Microelectrode study of marine snow and fecal pellets. Science **235:** 689–691.

———, and C. C. Gotschalk. 1988. In situ settling behavior of marine snow. Limnol. Oceanogr. **33:** 339–351.

———, C. C. Gotschalk, and S. MacIntyre. 1987. Evidence for sustained residence of macrocrustacean pellets in surface waters off southern California. Deep-Sea Res. **34:** 1641–1652.

———, and M. Silver. 1988. Characteristics, dynamics and significance of marine snow. Prog. Oceanog. **20:** 41–82.

Armstrong, R. A., C. Lee, J. I. Hedges, S. Honjo, and S. G. Wakeham. 2002. A new, mechanistic model for organic carbon fluxes in the ocean based on the quantitative association of POC with ballast minerals. Deep-Sea Res. I **49:** 219–236.

Azetsu-Scott, K., and U. Passow. 2004. Ascending marine particles: Significance of transparent exopolymer particles (TEP) in the upper ocean. Limnol. Oceanogr. **49:** 741–748.

Broecker, W. S., and T. H. Peng. 1974. Gas exchange rates between air and sea. Tellus **26:** 21–35.

Brzezinski, M. A., A. L. Alldredge, and L. M. O'Bryan. 1997. Silica cycling within marine snow. Limnol. Oceanogr. **42:** 1706–1713.

De La Rocha, C. L., and U. Passow. 2007. Factors influencing the sinking of POC and the efficiency of the biological carbon pump. Deep-Sea Res. II **54:** 639–658.

Dilling, L., and A. L. Alldredge. 2000. Fragmentation of marine snow by swimming macrozooplankton: A new process impacting carbon cycling in the sea. Deep-Sea Res. I **47:** 1227–1245.

Engel, A., and M. Schartau. 1999. Influence of transparent exopolymer particles on sinking velocity of *Nitzschia clostridium* aggregates. Mar. Ecol. Prog. Ser. **182:** 69–76.

Feinberg, L. R., and H. G. Dam. 1998. Effects of diet on dimensions, density and sinking rates of fecal pellets of the copepod *Acartia tonsa*. Mar. Ecol. Prog. Ser. **175:** 87–96.

Fenchel, T., and B. J. Finlay. 1993. Ecology and evolution in anoxic worlds. Oxford Univ. Press.

Fischer, G., and others. In press. Control of ballast minerals on organic carbon export in the Eastern Boundary Current System (EBCs) off NW Africa. *In* K.-K. Liu et al. [Eds.]. Carbon and nutrient fluxes in continental margins: A global synthesis. Springer.

Francois, R., S. Honjo, R. Krishfeld, and S. Manganini. 2002. Factors controlling the flux of organic carbon to the bathypelagic zone of the ocean. Global Biogeochem. Cycles **16:** 1087, doi: 10.1029/2001GB00172.

Guillard, J. K., and J. H. Ryther. 1962. Studies of marine planktonic diatoms. I. *Cyclotella nana* (Hustedt) and *Detonula confervacea* (Cleve) Gran. Can. J. Microbiol. **8:** 229–239.

Iversen, M. H., and L. Poulsen. 2007. Coprorhexy, coprophagy, and coprochaly in the copepods *Calanus helgolandicus*, *Pseudocalanus elongatus*, and *Oithona similis*. Mar. Ecol. Prog. Ser. **350:** 79–89.

Khelifa, A., and P. S. Hill. 2007. Models for effective density and settling velocity of flocs. J. Hydraul. Res. **44:** 390–401.

Kiørboe, T. 2001. Formation and fate of marine snow: Small-scale processes with large-scale implications. Sci. Mar. **65:** 57–71.

———, H.-P. Grossart, H. Ploug, and K. Tang. 2002. Mechanisms and rates of bacterial colonization of sinking aggregates. Appl. Environ. Microbiol. **68:** 3996–4006.

———, H. Ploug, and U. H. Thygesen. 2001. Fluid motion and solute distribution around sinking aggregates. I. Small scale fluxes and heterogeneity of nutrients in the pelagic environment. Mar. Ecol. Prog. Ser. **211:** 1–13.

Klaas, C., and D. E. Archer. 2002. Association of sinking organic matter with various types of mineral ballast in the deep sea: Implications for the rain ratio. Global Biogeochem. Cycles **16:** 1116, doi: 10.1029/2001GB001765.

Logan, B. E., and D. B. Wilkinson. 1990. Fractal geometry of marine snow and other biological aggregates. Limnol. Oceanogr. **35:** 130–136.

Müller, P. J., and R. Schneider. 1993. An automated leaching method for the determination of opal in sediments and particulate matter. Deep-Sea Res. I **40:** 425–444.

Ploug, H. 2001. Small-scale oxygen fluxes and remineralization in sinking aggregates. Limnol. Oceanogr. **46:** 1624–1631.

———. 2008. Cyanobacterial aggregates formed by *Aphanizomenon* sp. and *Nodularia spumigena* in the Baltic Sea: Small-scale fluxes, pH and oxygen microenvironments. Limnol. Oceanogr. **53:** 914–921.

———, and H.-P. Grossart. 2000. Bacterial growth and grazing on diatom aggregates: Respiratory carbon turnover as a function of aggregate size and sinking velocity. Limnol. Oceanogr. **45:** 1467–1475.

———, H.-P. Grossart, F. Azam, and B. B. Jørgensen. 1999. Photosynthesis, respiration, and carbon turnover in sinking marine snow from surface waters of Southern California Bight: Implications for the carbon cycle in the ocean. Mar. Ecol. Prog. Ser. **179:** 1–11.

———, S. Hietanen, and J. Kuparinen. 2002. Diffusion and advection within and around sinking, porous diatom aggregates. Limnol. Oceanogr. **47:** 1129–1136.

———, M. H. Iversen, M. Koski, and E. T. Buitenhuis. 2008. Production, respiratory carbon turnover, and sinking velocity of copepod fecal pellets: Direct measurements of ballasting by opal and calcite. Limnol. Oceanogr. **53:** 469–476.

———, and B. B. Jørgensen. 1999. A net-jet flow system for mass transfer and microelectrode studies in sinking aggregates. Mar. Ecol. Prog. Ser. **176:** 279–290.

———, M. Kühl, B. Bucholz, and B. B. Jørgensen. 1997. Anoxic aggregates—an ephemeral phenomenon in the pelagic environment. Aquat. Microb. Ecol. **13:** 285–294.

———, and U. Passow. 2007. Direct measurements of diffusivity in diatom aggregates containing transparent exopolymer particles (TEP). Limnol. Oceanogr. **52:** 1–6.

Revsbech, N. P. 1989. An oxygen microelectrode with a guard cathode. Limnol. Oceanogr. **34:** 474–478.

———, L. P. Nielsen, and N. B. Ramsing. 1998. A novel microsensor for determination of apparent diffusivity in sediments. Limnol. Oceanogr. **43:** 986–992.

Schwinghamer, P., D. M. Anderson, and D. M. Kulis. 1991. Separation and concentration of living dinoflagellate resting cysts from marine sedimentation via density-gradient centrifugation. Limnol. Oceanogr. **36:** 588–592.

Shanks, A. L., and E. W. Edmondson. 1989. Laboratory-made artificial marine snow: A biological model of the real thing. Mar. Biol. **101:** 463–470.

———, and J. D. Trent. 1979. Marine snow: Microscale nutrient patches. Limnol. Oceanogr. **24:** 850–854.

Simon, M., H.-P. Grossart, B. Schweitzer, and H. Ploug. 2002. Microbial ecology of organic aggregates in aquatic ecosystems. Review. Aquat. Microb. Ecol. **28:** 175–211.

Smith, D. C., M. Simon, A. L. Alldredge, and F. Azam. 1992. Intense hydrolytic enzyme activity on marine aggregates and implication for rapid particle dissolution. Nature **359:** 139–142.

Thor, P., H. G. Dam, and D. R. Rogers. 2003. Fate of organic carbon release from decomposing copepod fecal pellets in relation to bacterial production and ectoenzymatic activity. Mar. Ecol. Prog. Ser. **33:** 279–288.

Turner, J. T. 2002. Zooplankton fecal pellets, marine snow and sinking phytoplankton blooms. Aquat. Microb. Ecol. **27:** 57–102.

Wakeham, S. G., and others. 1980. Organic-matter fluxes from sediment traps in the equatorial Atlantic Ocean. Nature **286:** 798–800.

Weast, R. C. 1968. Handbook of chemistry and physics, 49th ed. CRC Co.

White, F. M. 1974. Viscous fluid flow. McGraw-Hill.

Ziervogel, K., and C. Arnosti. 2008. Polysaccharide hydrolysis in aggregates and free enzyme activity in aggregate-free seawater from the north-eastern Gulf of Mexico. Environ. Microbiol. **10:** 289–299.

Received: 14 November 2007
Accepted: 28 February 2008
Amended: 10 April 2008